SpoT-Mediated NapA Upregulation Promotes Oxidative Stress-Induced *Helicobacter pylori* Biofilm Formation and Confers Multidrug Resistance

Yican Zhao,[a] Yuying Cai,[a] Zhenghong Chen,[b] Huanjie Li,[a] Zhengzheng Xu,[a] Wenjuan Li,[a] Jihui Jia,[a] ⓘ Yundong Sun[a]

[a]Key Laboratory for Experimental Teratology of the Ministry of Education and Department of Microbiology, School of Basic Medical Science, Cheeloo College of Medicine, Shandong University, Jinan, Shandong, China
[b]Department of Microbiology, Key Laboratory of Medical Microbiology and Parasitology, Guizhou Medical University, Guiyang, China

Yican Zhao, Yuying Cai, Zhenghong Chen, and Huanjie Li contributed equally to this work. Author order was determined by drawing straws.

ABSTRACT Recently, the incidence of drug-resistant *Helicobacter pylori* infection has increased. Biofilm formation confers multidrug resistance on bacteria. Moreover, it has been found that the formation of biofilms on the surfaces of gastric mucosae is an important reason for the difficulty of eradication of *H. pylori*. The mechanisms underlying *H. pylori* biofilm formation *in vivo* have not been elucidated. Reactive oxygen species (ROS) released by the host immune cells in response to *H. pylori* infection cannot effectively clear the pathogen. Moreover, the extracellular matrix of the biofilm protects the bacteria against ROS-mediated toxicity. This study hypothesized that ROS can promote *H. pylori* biofilm formation, and treatment with low concentrations of hydrogen peroxide (H_2O_2) promoted this process *in vitro*. Comparative transcriptome analysis of planktonic and biofilm-forming cells revealed that the expression of SpoT, a (p)ppGpp (guanosine 3′-diphosphate 5′-triphosphate and guanosine 3′,5′-bispyrophosphate) synthetase/hydrolase, is upregulated in H_2O_2-induced biofilms and that knockout of *spoT* inhibited *H. pylori* biofilm formation. Additionally, this study used weighted gene coexpression network analysis to examine the key target molecules involved in SpoT regulation. The analysis revealed that neutrophil-activating protein (NapA; HP0243) promoted H_2O_2-induced biofilm formation and conferred multidrug resistance. Furthermore, vitamin C exhibited anti-*H. pylori* biofilm activity and downregulated the expression of *napA in vitro*. These findings provide novel insights into the clearance of *H. pylori* biofilms.

KEYWORDS *Helicobacter pylori*, biofilms, antibiotic resistance, SpoT, NapA

Globally, the average infection rate of *Helicobacter pylori*, a common pathogen, is approximately 50%. In some areas of developing countries, the infection rate is as high as 90% (1). Previous studies have demonstrated that *H. pylori* infection is associated with chronic gastritis, peptic ulcer, and gastric cancer (2). Thus, the alleviation of *H. pylori* infection can aid in decreasing the incidence of gastric cancer (3).

However, the major challenge for the alleviation of *H. pylori* infection is the development of drug resistance in the pathogen (4). Biofilm formation confers drug resistance on *H. pylori* (5–7), especially against common clinical antibiotics. For example, the MICs of clarithromycin, amoxicillin, and metronidazole against *H. pylori* biofilms were 40-, 40-, and 10-fold higher, respectively, than those against planktonic bacteria (8).

In 2006, Carron and colleagues first reported that *H. pylori* could form biofilms on the gastric mucosal surface, as determined by using scanning electron microscopy (SEM) (9). The rate of *H. pylori* biofilm formation on the gastric mucosae of patients with peptic ulcers was 97.3% (10). Cammarota et al. reported that the efficacy of

antibiotics against *H. pylori* biofilms on the gastric mucosae was at least 4 times lower than that against planktonic cells in all patients (11).

Recent studies have demonstrated that *H. pylori* forms biofilms on the surfaces and in the compartments of the human gastric glands (12). However, the mechanism underlying *H. pylori* biofilm formation in the stomach has not been elucidated. The elucidation of mechanisms underlying biofilm formation can aid in developing therapeutic strategies to inhibit *H. pylori* biofilm formation *in vivo* and treat refractory *H. pylori* infections.

Host immune cells secrete reactive oxygen species (ROS) as the first line of defense against pathogens (13). *H. pylori* infection elicits a strong inflammatory response upon colonization of the host gastric mucosa. The host inflammatory response is mediated mainly by neutrophils and macrophages, which release ROS and reactive nitrogen species to eliminate *H. pylori* (14–17).

However, *H. pylori* can permanently colonize the gastric mucosa, a process mediated through various oxidoreductase systems (18). Biofilms protect the bacteria against the toxic effects of ROS produced by the host immune cells (19). The extracellular matrix of *H. pylori* is a physical barrier that prevents the diffusion of ROS (20).

Meta-analysis of clinical treatment data has revealed that combination treatment with antioxidants and antibiotics increased the clearance rate of *H. pylori* (21). This may be attributed to the effects of antioxidants on biofilms. For example, studies have found that vitamin C (Vc) can destabilize bacterial biofilms (22).

These findings suggested that ROS released from the inflammatory cells promote the formation of *H. pylori* biofilms in the stomach. In this study, the formation of *H. pylori* biofilms was induced *in vitro* using a low concentration of hydrogen peroxide (H_2O_2). Additionally, the mechanism underlying H_2O_2-induced biofilm formation was examined using transcriptome sequencing.

RESULTS

Oxidative stress promotes *H. pylori* biofilm formation. Based on previous studies examining the effects of ROS on bacteria (23, 24), an *H. pylori* culture was supplemented with low concentrations of H_2O_2 to simulate the oxygen stress environment encountered by *H. pylori* in the human body. The effect of oxidative stress on the induction of *H. pylori* biofilm formation was examined. Supplementation with $50\,\mu M$ H_2O_2 promoted biofilm formation in *H. pylori* strain 26695 (the wild-type [WT] strain) and the clinical isolate strain (strain H57) (Fig. 1).

We also found that biofilms induced by H_2O_2 were more tolerant to antibiotics than those we had previously induced through nutrient deficiency (see Table S1 in the supplemental material).

Analysis of differentially expressed genes involved in *H. pylori* biofilm formation using transcriptome sequencing. To analyze the mechanism underlying H_2O_2-induced *H. pylori* biofilm formation, the transcriptomes of the planktonic WT strain (WtP) and the biofilm-forming WT strain (WtB) were comparatively analyzed. The transcriptome data were represented as a heat map (Fig. 2A).

The genes that were differentially expressed in the WtB and WtP strains were analyzed using a volcano plot (Fig. 2B). In total, 152 differentially expressed genes were identified. Analysis with the KEGG GENES database revealed that the differentially expressed genes can be classified into various functional components, including metabolism and enzymes (25), ribosomal proteins (8), oxidoreductases (7), regulatory genes (1), and transporters (efflux pumps) (Fig. 2C).

The stress response gene *spoT* (HP0775) is shown on the volcano plot (Fig. 2B). *spoT* encodes (p)ppGpp synthase/hydrolase (26). (p)ppGpp, which was first discovered in *Escherichia coli* by Michael Cashel in the 1960s (27), is involved in the regulation of the bacterial stringent/stress response. The stress response is an adaptive regulatory response of bacteria to stressful environments, such as nutritional deficiency, heat stress, and antibiotics (26).

The formation of biofilms is a bacterial stress response (28). Hence, we hypothesized

A WT H57

B
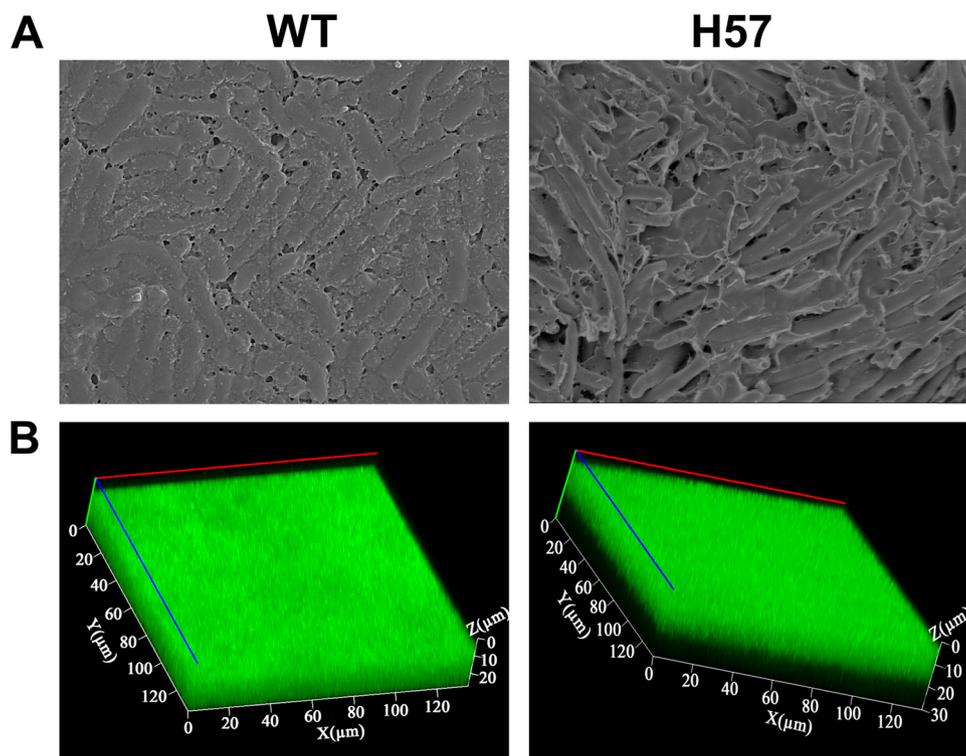
FIG 1 A low concentration of H_2O_2 (50 μM) promotes biofilm formation in the wild-type and H57 *Helicobacter pylori* strains. (A) Confocal laser scanning microscopy images of the biofilm. Cells stained with membrane-permeant SYTO 9 (green) and membrane-impermeant propidium iodide (red) were visualized using confocal microscopy. (B) Scanning electron microscopy images of the biofilm. The biofilm used in this experiment is a mature biofilm grown on a nitrocellulose membrane for 3 days. The planktonic bacteria were from the early-exponential phase (OD_{600}, 0.4 to 0.5).

that SpoT may play an important role in the oxidative stress-induced formation of *H. pylori* biofilms.

SpoT promotes oxidative stress-induced *H. pylori* biofilm formation and confers multidrug resistance. The levels of SpoT expression in H_2O_2-induced biofilms of the WT and H57 strains were examined using quantitative real-time PCR (qRT-PCR). The results showed that *spoT* was upregulated in biofilm-forming cells from both the WT and H57 strains relative to expression in planktonic cells (Fig. 3A).

To further verify the level of SpoT expression in biofilms, the levels of ppGpp and pppGpp expression in planktonic and biofilm-forming cells of the WT and H57 strains were examined using a ^{32}P-postlabeling/thin-layer chromatography (^{32}P-TLC) assay (Fig. 3B). Relative to those in planktonic cells, the expression levels of ppGpp and pppGpp were significantly upregulated in biofilm-forming cells.

These results indicate that SpoT is involved in the oxidative stress-induced formation of *H. pylori* biofilms. Additionally, a *spoT* knockout strain (ΔspoT) and a complemented strain (spoT*) were constructed in order to comparatively analyze the biofilm-forming abilities of the ΔspoT, spoT*, and WT strains (Fig. 3C and D). As shown in Fig. 3C and D, the ΔspoT strain could not form a complete biofilm. Moreover, the biofilm-forming ability of the spoT* strain was similar to that of the WT strain.

Next, the susceptibilities of WT, ΔspoT, and spoT* biofilms to multiple antibiotics were comparatively analyzed (Table S1). The MIC value of penicillin G against the ΔspoT strain was 30-fold lower than that against the WT strain. The MIC value of tetracycline hydrochloride against the WT strain was 8-fold lower than that against the ΔspoT strain. Additionally, the MIC values of various antibiotics for the spoT* and WT strains were similar.
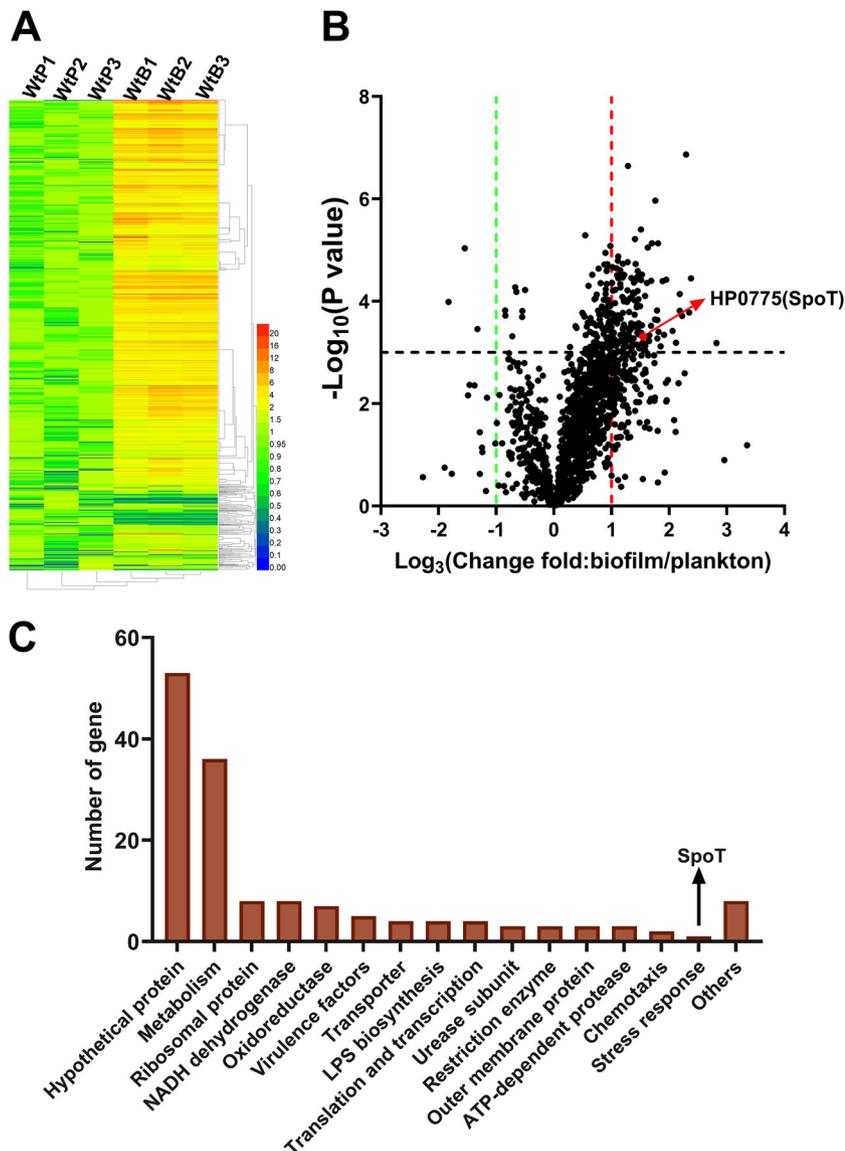
FIG 2 Analysis of differentially expressed genes in biofilms and planktonic cells of the wild-type *Helicobacter pylori* strain. (A) Heat map of transcripts expressed in biofilms ($n = 3$) and planktonic cells ($n = 3$). (B) Volcano plot analysis of expressed transcripts to identify the differentially expressed genes. (C) Functional classification of differentially expressed genes according to the KEGG GENES database. The number of annotated genes (y axis) is plotted against the KEGG categories (x axis). LPS, lipopolysaccharide.

WGCNA modules associated with *H. pylori* biofilm formation and SpoT. The biofilm-forming cells and planktonic cells of the $\Delta spoT$ strain ($\Delta spoT$B and $\Delta spoT$P cells, respectively) were also subjected to transcriptome sequencing. The transcriptome data of these cells were compared with those of the WT strain. Weighted gene coexpression network analysis (WGCNA) of 1,526 genes (Fig. S1) revealed 25 modules (Fig. 4A and B). Correlation analysis revealed that the "red" module, containing 62 genes, was correlated with *spoT* ($r = 0.87$; $P = 9.0 \times 10^{-7}$) and biofilm formation ($r = 0.87$; $P = 9.0 \times 10^{-7}$) (Fig. 4B). Therefore, these 62 SpoT-regulated genes in the "red" module were considered to play an important role in the oxidative stress-induced formation of *H. pylori* biofilms.

Cytoscape network visualization of 27 genes with WGCNA edge weights of >0.10 indicated that these genes are highly correlated. Of the 27 genes, 23 had five or more

A

B

C

D
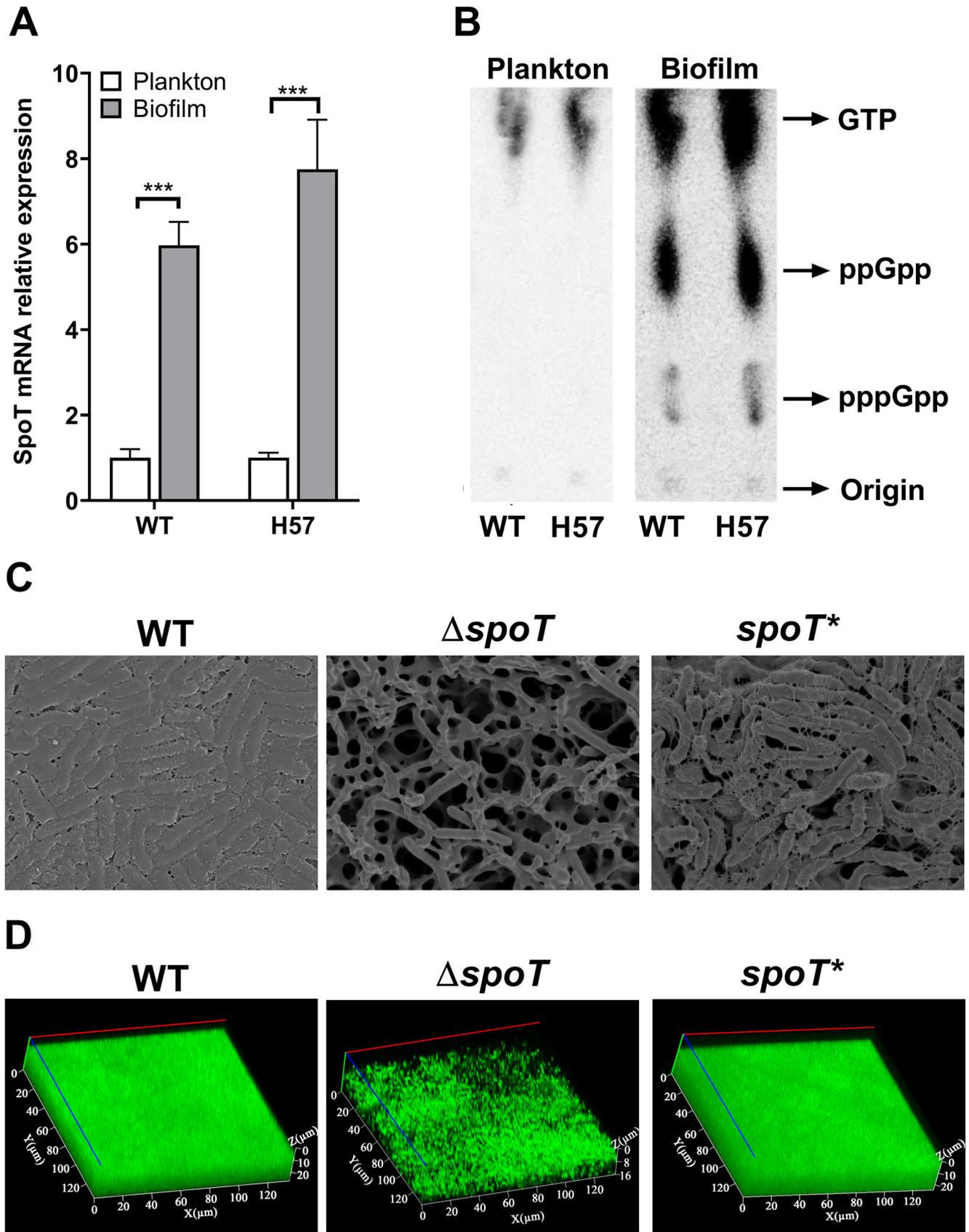
FIG 3 SpoT is involved in the H_2O_2-induced formation of biofilms by the *Helicobacter pylori* wild-type (WT) and H57 strains. (A) Levels of *spoT* mRNA expression in biofilm-forming and planktonic cells were examined using quantitative real-time PCR. The expression levels of target genes were

A   Gene dendrogram and module colors

B   Module Trait Relationships

C
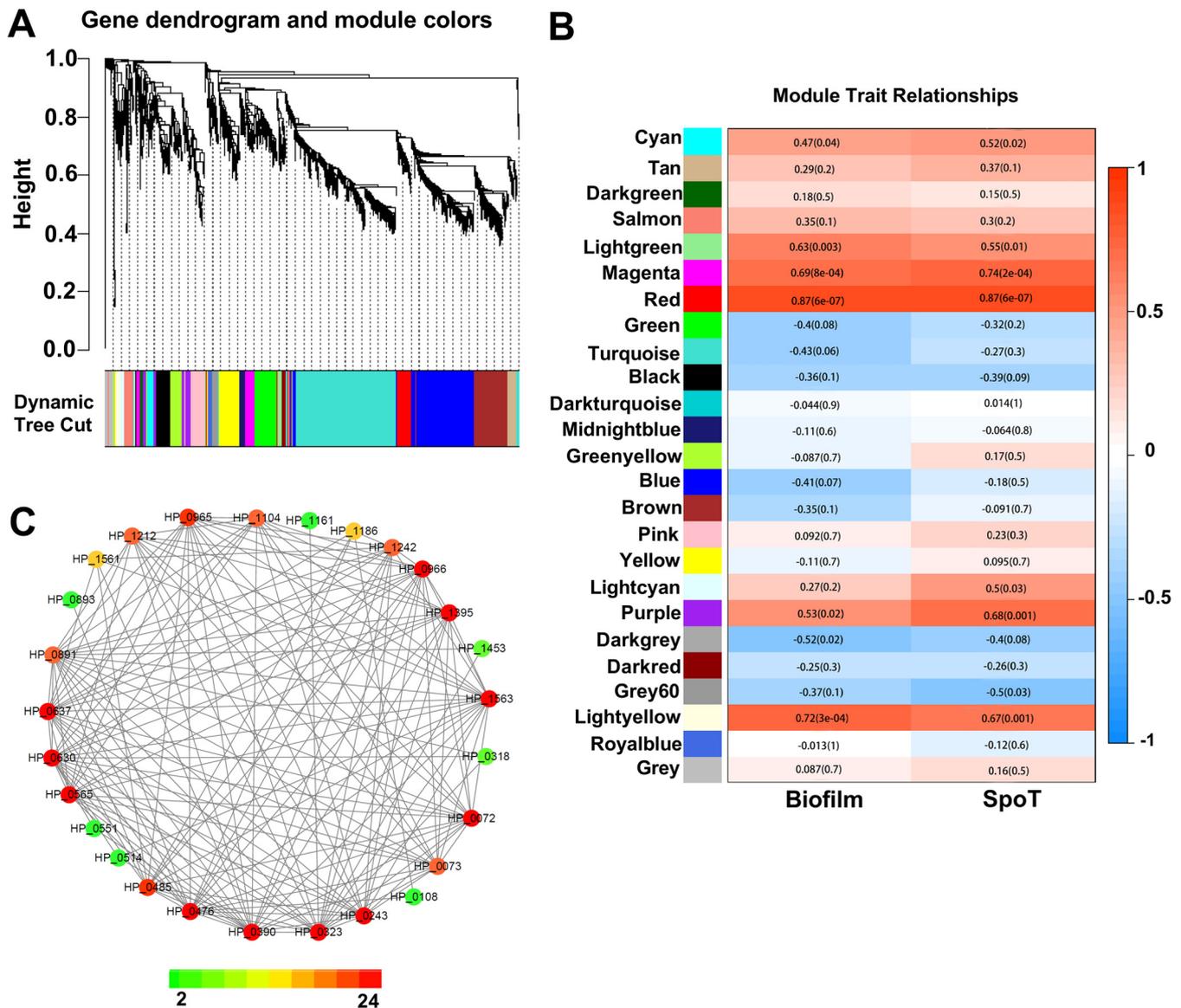
FIG 4 Weighted gene coexpression network analysis of genes that are differentially expressed in the biofilm-forming and planktonic cells of the wild-type (WT) and Δ*spoT* strains. (A) (Top) Hierarchical cluster tree showing 25 modules of coexpressed genes. Each differentially expressed gene is represented as a leaf on the tree, while each of the 25 modules is represented as a tree branch. (Bottom) Modules shown in colors (such as tan, red, and yellow) designated in panel B. (B) (Left) The 25 modules. (Center) Correlation between modules and SpoT/biofilm weight (with the corresponding *P* values shown in parentheses). (Right) Color scale showing module-trait correlation from −1 (blue) to 1 (red). (C) Cytoscape representation of coexpressed genes with edge weights of ≥0.10 in the "red" module. The number of edges of the genes ranges from 4 to 24 (color-coded from green through red according to the scale on the bottom). Member gene identifications are shown.

edges, while only 4 genes (*hp0893*, *hp1453*, *hp0318*, and *hp0108*) had low edge numbers (Fig. 4C).

Additionally, the "magenta" module, with 53 genes, and the "light yellow" module, with 43 genes, were correlated with *H. pylori* biofilm formation and SpoT. However, the

FIG 3 Legend (Continued)
normalized to those of 16S rRNA genes. Data are presented as means ± standard errors of the means from three independent experiments. Asterisks indicate significance by an unpaired Student *t* test (***, *P* <0.001). (B) The expression of (p)ppGpp (guanosine 3′-diphosphate 5′-triphosphate and guanosine 3′,5′-bispyrophosphate) was upregulated in biofilm-forming cells of the WT and H57 strains but not in planktonic cells. ^{32}P-labeled nucleotides of formic acid extracts of *H. pylori* were detected using thin-layer chromatography. Planktonic *H. pylori* bacteria were cultured to the exponential phase. (C) Scanning electron microscopy images of WT, Δ*spoT*, and *spoT** biofilms. In this experiment, a mature biofilm grown on a nitrocellulose membrane for 3 days was used. The planktonic bacteria were from the early-exponential-phase culture (OD$_{600}$, 0.4 to 0.5). (D) Confocal laser scanning microscopy images of WT, Δ*spoT*, and *spoT** biofilms. Cells stained with membrane-permeant SYTO 9 (green) and membrane-impermeant propidium iodide (red) were visualized using confocal microscopy.

TABLE 1 Genes that may be involved in *H. pylori* biofilm formation and regulated by SpoT, according to WGCNA analysis[a]

Classification according to function	Predicted function	Locus tag
Outer membrane protein	Outer membrane protein (*omp30*)	HP_1395
ABC transporter	Iron(III) ABC transporter, periplasmic iron-binding protein (*ceuE*)	HP_1561
Oxidoreductase	DNA protection during starvation protein	HP_0243
	Cinnamyl-alcohol dehydrogenase ELI3-2 (*cad*)	HP_1104
	Flavodoxin (*fldA*)	HP_1161
	Catalase-like protein	HP_0485
	Alkyl hydroperoxide reductase (*tsaA*)	HP_1563
	Adhesin-thiol peroxidase (*tagD*)	HP_0390
	NADPH quinone reductase, modulator of drug activity (*mda66*)	HP_0630
Hydrolase	Urease subunit beta	HP_0072
	Urease subunit alpha	HP_0073
Genetic information processing	Glutamyl-tRNA synthetase (*gltX1*)	HP_0476
Metabolism	F_oF_1 ATP synthase subunit C (*atpE*)	HP_1212
Ribosomal protein	50S ribosomal protein L9	HP_0514
	50S ribosomal protein L31	HP_0551
Hypothetical protein	Hypothetical protein	HP_0108
	Hypothetical protein	HP_0318
	Hypothetical protein	HP_0565
	Hypothetical protein	HP_0637
	Hypothetical protein	HP_0891
	Hypothetical protein	HP_0893
	Hypothetical protein	HP_0965
	Hypothetical protein	HP_0966
	Hypothetical protein	HP_1453

[a]See Fig. 4C.

correlations of the "magenta" and "light yellow" modules with biofilm formation and SpoT were lower than that of the "red" module.

According to the functional annotation of genes in the KEGG GENES database, 27 genes with WGCNA edge weights of >0.10 in the "red" module can be divided into eight categories, including outer membrane proteins, ABC transporters, oxidoreductases, and hydrolases (Table 1).

Screening the key target genes involved in SpoT-regulated biofilm formation. To further identify the key target genes involved in SpoT-regulated biofilm formation, the expression levels of nine key genes in the WT and H57 strains were analyzed using qRT-PCR (Table 2). These genes were functionally classified as outer membrane proteins, ABC transporters, and oxidoreductases, which may be involved in biofilm formation.

As shown in Table 2, for the WT strain, the expression levels of two genes (*hp0243* [*napA*]) and *hp1161*) in biofilm-forming cells were upregulated by >4-fold over those in planktonic cells. In addition, for the H57 strain, the expression levels of the nine key genes in biofilm-forming cells were upregulated over those in planktonic cells, and the expression of *napA* was significantly upregulated, by >7-fold (Table 2). The fact that *napA* expression in biofilm-forming cells of both the WT and H57 strains was upregulated by >4-fold over that in planktonic cells indicates that *napA* may be involved in biofilm formation under oxidative stress conditions.

SpoT regulates *napA* expression. The role of *spoT* in regulating *napA* expression was examined by comparatively analyzing the expression levels of *napA* in biofilm-forming cells of the WT, Δ*spoT*, and *spoT** strains (Fig. 5A). *napA* expression was upregulated in the WT and *spoT** strains on the third, fourth, and fifth days of biofilm formation. Additionally, *napA* expression was highest on the fourth day of biofilm formation in these strains but was not detected in the Δ*spoT* strain (Fig. 5A).

Previously, we had demonstrated that clarithromycin (CLA) could promote *spoT* expression (29). To examine the regulation of *spoT* expression by *napA*, the WT, Δ*spoT*, and *spoT** strains were treated with different concentrations of CLA (0.25, 0.5, and 1 μg/ml) for 30 min. *napA* expression levels were examined using qRT-PCR. Treatment

TABLE 2 qRT-PCR analysis of the relative gene expression difference between biofilm-forming and planktonic cells in the WT and H57 strains

| Locus tag | Predicted function | BF/PKC fold change[a] in the following strain: | |
		WT	H57
HP_0243	DNA protection during starvation protein (napA)	4.62 ± 0.41***	7.52 ± 0.26***
HP_1104	Cinnamyl-alcohol dehydrogenase ELI3-2 (cad)	1.17 ± 0.10	5.60 ± 0.16**
HP_1161	Flavodoxin (fldA)	4.35 ± 0.38***	2.98 ± 0.32**
HP_0485	Catalase-like protein	2.00 ± 0.06***	3.27 ± 0.30***
HP_1563	Alkyl hydroperoxide reductase (tsaA)	1.59 ± 0.12**	2.44 ± 0.92
HP_0390	Adhesin-thiol peroxidase (tagD)	1.68 ± 0.08	4.54 ± 0.54***
HP_0630	Modulator of drug activity (mda66)	2.74 ± 0.27***	4.98 ± 0.46**
HP_1395	Outer membrane protein (omp30)	0.59 ± 0.02**	4.60 ± 0.11***
HP_1561	Iron(III) ABC transporter, periplasmic iron-binding protein (ceuE)	1.18 ± 0.08	2.13 ± 0.31**

[a]BF, biofilm-forming cells; PKC, planktonic cells. P values are indicated by asterisks as follows: **, $P < 0.01$; ***, $P < 0.001$.

with 0.25 μg/ml of CLA was considered an optimal condition to induce napA expression in the WT and spoT* strains but not in the ΔspoT strain (Fig. 5B).

Next, napA expression levels in the WT, ΔspoT, and spoT* strains treated with 0.25 μg/ml CLA for 10, 20, or 30 min were examined using qRT-PCR. CLA time-dependently upregulated napA expression in the WT and spoT* strains. In contrast, CLA did not upregulate napA expression in the ΔspoT strain (Fig. 5C).

NapA promotes H. pylori biofilm formation and confers multidrug resistance. Previous studies have demonstrated that napA can protect H. pylori against oxidative stress (30), suggesting that napA may be involved in the oxidative stress-induced formation of H. pylori biofilms. The formation of biofilms in the WT, napA knockout (ΔnapA), and napA complementation (napA*) strains was analyzed using SEM. Compared with the WT and napA* biofilms, the ΔnapA biofilm exhibited loose bacterial arrangement, incomplete extracellular matrix formation, a higher number of cavities, and a spherical shape. The results of confocal laser scanning microscopy (CLSM) analysis and a LIVE/DEAD cell viability assay revealed that the ΔnapA strain formed a thin biofilm (Fig. 6).

Next, we compared the growth curves of the WT, ΔnapA, and napA* strains and found that napA knockdown did not affect the growth of H. pylori (Fig. S2). Analysis of the MIC values of various antibiotics revealed that the ΔnapA strain was more sensitive to antibiotics, such as amoxicillin, clarithromycin, and tetracycline, than the WT and napA* strains (Table 3).

The viabilities of the three strains on plates supplemented with different antibiotics were comparatively analyzed. The number of clones formed by the ΔnapA strain was significantly lower than the numbers formed by the WT and napA* strains (Fig. 7).

napA knockout promotes oxidative stress-induced H. pylori genomic DNA damage. Previous studies have reported that napA can protect H. pylori against oxidative stress-induced genomic DNA damage. (31). Hence, DNA damage and fragmenta-
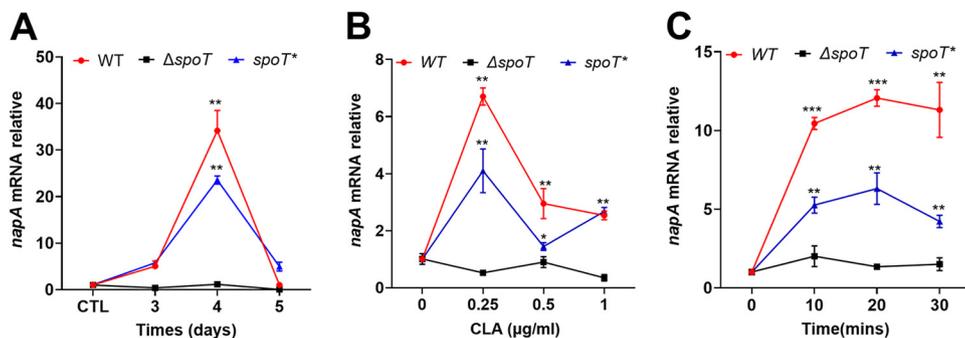
FIG 5 napA mRNA expression levels in the wild-type (WT), ΔspoT, and spoT* strains. (A) Expression of napA in the biofilms of the WT, ΔspoT, and spoT* strains for different durations. The planktonic cells served as a control. (B and C) Expression levels of napA in the WT, ΔspoT, and spoT* strains treated with different concentrations of clarithromycin (CLA) for 30 min (B) or with 0.25 μg/ml CLA for various durations (C).

A

WT   ΔnapA   napA*

B
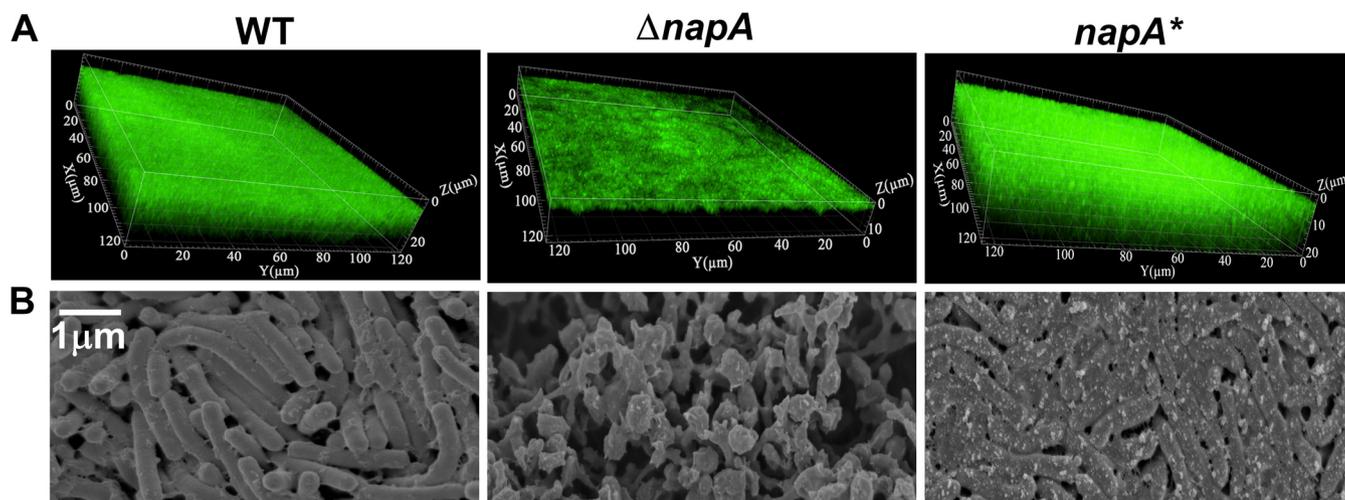
FIG 6 NapA is involved in the H_2O_2-induced formation of *Helicobacter pylori* biofilms. (A) Confocal laser scanning microscopy images of wild-type (WT), Δ*napA*, and *napA** biofilms. Cells stained with membrane-permeant SYTO 9 (green) and membrane-impermeant propidium iodide (red) were visualized using confocal microscopy. (B) Scanning electron microscopy images of WT, Δ*napA*, and *napA** biofilms. In this experiment, a mature biofilm grown on a nitrocellulose membrane for 3 days was used. The planktonic bacteria were from the early-exponential-phase culture (OD_{600}, 0.4 to 0.5).

tion in the WT, Δ*napA*, and *napA** biofilms were examined using electrophoresis (Fig. 8). The DNA fragmentation level was low in the WT strain, with 4 kb as the smallest fragment size. In contrast, the Δ*napA* strain exhibited significantly high levels of DNA fragmentation, and the size of the smallest fragment was approximately 1 kb. This indicated that relative to the WT strain, the Δ*napA* strain exhibited enhanced oxidative stress-induced genomic DNA damage.

Vc and NAC exhibit anti-*H. pylori* biofilm activity and downregulate *napA* expression. Next, we hypothesized that antioxidants may exhibit anti-*H. pylori* biofilm activity. In this study, the effects of various concentrations of antioxidants (32), such as baicalin, anthocyanins, vitamin C (Vc), and *N*-acetylcysteine (NAC), on *H. pylori* biofilms were examined. Baicalin exhibited weak anti-*H. pylori* biofilm activity. At a concentration of 112 µg/ml, baicalin could not decrease the biofilm mass by 50% (Fig. 9A). However, anthocyanins decreased the biofilm mass by >50% at treatment concentrations higher than 80 µg/ml (Fig. 9B).

Vc exhibited potent antibiofilm activity. At concentrations higher than 30 mM, Vc decreased the biofilm mass by >50% (Fig. 9C). NAC exhibited the strongest anti-*H. pylori* biofilm activity. Treatment with 2.5 mg/ml NAC decreased the biofilm mass by >50% (Fig. 9D). SEM analysis revealed that treatment with 5 mg/ml NAC resulted in almost complete loss of the extracellular matrix of the *H. pylori* biofilm (Fig. 10A). Similarly, treatment with 40 mM Vc resulted in the loss of the *H. pylori* biofilm extracellular matrix (Fig. 10B).

This study demonstrated that NapA regulates the oxidative stress-induced formation of *H. pylori*. Hence, *napA* mRNA expression levels in the Vc-treated and NAC-

TABLE 3 MICs determined for the WT, Δ*napA*, and *napA** strains in biofilm-forming and planktonic cells

Drug	MIC (µg/ml) for the following type of cells:					
	Planktonic			Biofilm forming		
	WT	Δ*napA*	*napA**	WT	Δ*napA*	*napA**
Amoxicillin	0.0625	0.0156	0.03125	5	2	5
Clarithromycin	0.0625	0.0078	0.0156	6.25	1	4
Penicillin G	0.0625	0.0156	0.0625	8	1	8
Tetracycline	0.125	0.03125	0.0625	10	2	8
Metronidazole	0.5	0.125	0.25	16	1	12
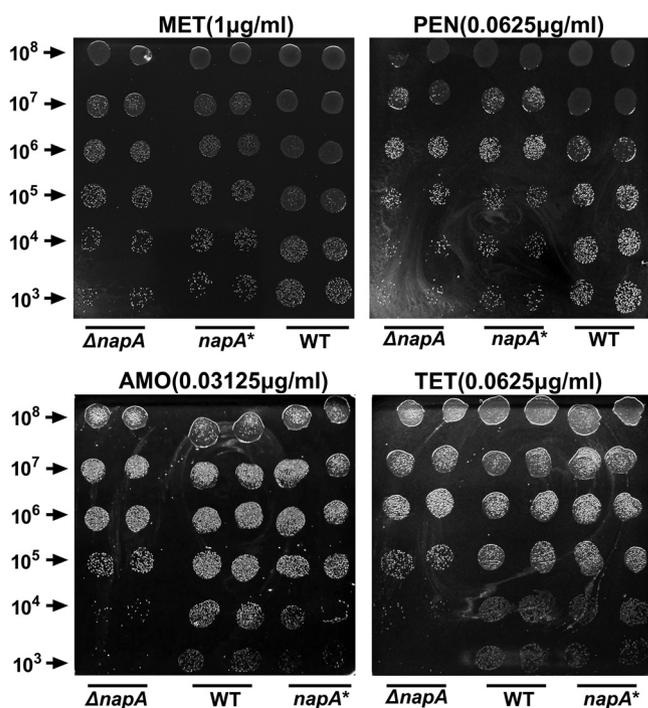
FIG 7 Effects of different antibiotics on the colony-forming abilities of the wild-type, Δ*napA*, and *napA** strains. Serially diluted bacterial cultures were spotted onto Mueller-Hinton agar plates, and their colony-forming abilities in the presence of different antibiotics (metronidazole [MET], penicillin [PEN], amoxicillin [AMO], and tetracycline [TET]) were assessed after 3 days. The experiments were performed in triplicate, and representative examples are shown.

treated groups were examined. Vc and NAC downregulated the expression of *napA* (Fig. 11).

DISCUSSION

The incidence of drug resistance in *H. pylori* has increased in recent years. The formation of biofilms *in vivo* contributes to the development of multidrug resistance in *H. pylori* (5). Previous studies have demonstrated that a low concentration of ROS can activate the stress response mechanism of bacteria and consequently promote biofilm formation (33). In this study, H_2O_2-induced oxidative stress promoted the formation of *H. pylori* biofilms. SpoT positively regulated the expression of NapA and the oxidative stress-induced formation of *H. pylori* biofilms. Furthermore, *N*-acetylcysteine and Vc exhibited anti-*H. pylori* biofilm activity and downregulated *napA* expression.

Stress conditions, such as subinhibitory concentrations of antibiotics (34), amino acid starvation (35), and oxidative stress (28), promote the formation of biofilms in bacteria. For example, enhanced levels of Fe^{3+} can promote the production of ROS in the host and the formation of biofilms in *Pseudomonas aeruginosa* (36). Free radicals and ROS in cigarette smoke promoted the formation of *Staphylococcus aureus* biofilms (25). Endogenous H_2O_2 can stimulate the formation of *Acinetobacter baumannii* biofilms (33).

In this study, H_2O_2 did not affect the growth of planktonic bacteria at concentrations lower than 50 μM. This indicated that a low concentration of H_2O_2 does not affect the viability of *H. pylori* and cannot promote the formation of biofilms. At concentrations higher than 200 μM, H_2O_2 markedly inhibited the growth of *H. pylori* and the formation of biofilms. In this study, the optimal concentration range of H_2O_2 for inducing biofilm formation in *H. pylori* was determined to be 50 to 200 μM.

In-Ae Jang et al. demonstrated that treatment with 100 μM H_2O_2 promoted the formation of biofilms in *Acinetobacter oleivorans* DR1 (33). Excessive H_2O_2 (usually ≥50 μM) is cytotoxic to various animals, plants, and bacterial cell cultures (37).
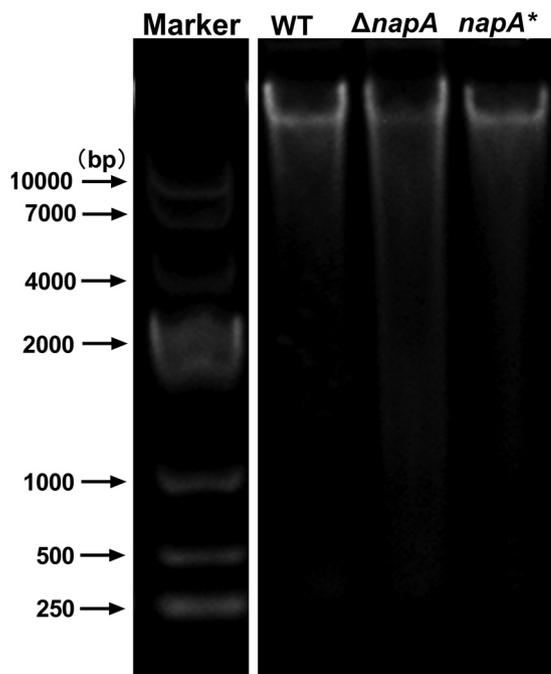
FIG 8 Agarose gel electrophoretic analysis of genomic DNA fragmentation in wild-type, Δ*napA*, and *napA** cells. The sizes of DNA standards are shown on the left. The experiments were repeated three times and yielded similar results.

Therefore, this study treated bacterial cultures with H_2O_2 at a final concentration of 50 μM to simulate the physiological environment. Supplementation of the culture medium with 50 μM H_2O_2 promoted biofilm formation in the WT and H57 strains of *H. pylori*.

Various reductase systems of *H. pylori* are involved in scavenging ROS (18). Additionally, biofilm formation protects against ROS-mediated toxic effects on bacteria. Bacteria are enclosed within the extracellular matrix, which can inhibit ROS diffusion, after biofilm formation (19). In this study, *H. pylori* formed biofilms with a dense extracellular matrix upon stimulation with low concentrations of H_2O_2.

Genes involved in oxidative stress regulation in other bacteria, such as *oxyR*, *soxR*, *soxS*, *rpoS*, *lexA*, and *perR* (18), were not detected in the *H. pylori* genome. Some oxidative stress-regulatory genes, such as *oxyR* and *rpoS* (19), can also regulate the formation of bacterial biofilms. The genes that regulate the oxidative stress response in *H. pylori* include the cytoplasmic chemoreceptor (TlpD) (38, 39), iron uptake regulation (*fur*) (30), posttranscriptional regulation (*csrA*) (40), and stress regulation (*spoT*) genes (41).

In this study, SpoT expression was upregulated in oxidative stress-induced biofilms. In most bacteria, (p)ppGpp is synthesized by RelA and SpoT (42). However, analysis of the *H. pylori* genome revealed that it lacks the gene encoding RelA and contains only the gene encoding SpoT (43). This indicates that (p)ppGpp is synthesized by SpoT in *H. pylori*.

SpoT is reported to be involved in the adaptive response of *H. pylori* to various stress conditions, such as amino acid starvation, an acidic environment, or an oxidative stress environment (41, 44). Recently, we demonstrated that SpoT is involved in the regulation of *H. pylori* tolerance to multiple antibiotics and that biofilm formation is induced under nutrient starvation conditions (8). Additionally, recent studies have demonstrated that (p)ppGpp regulates the formation of biofilms in other bacteria, such as *Enterococcus faecalis* (45), *Bordetella pertussis* (46), and *Vibrio cholerae* (47). Inhibition of (p)ppGpp is reported to suppress bacterial biofilm formation (48).

In this study, SpoT expression was upregulated in H_2O_2-induced biofilm cells. The
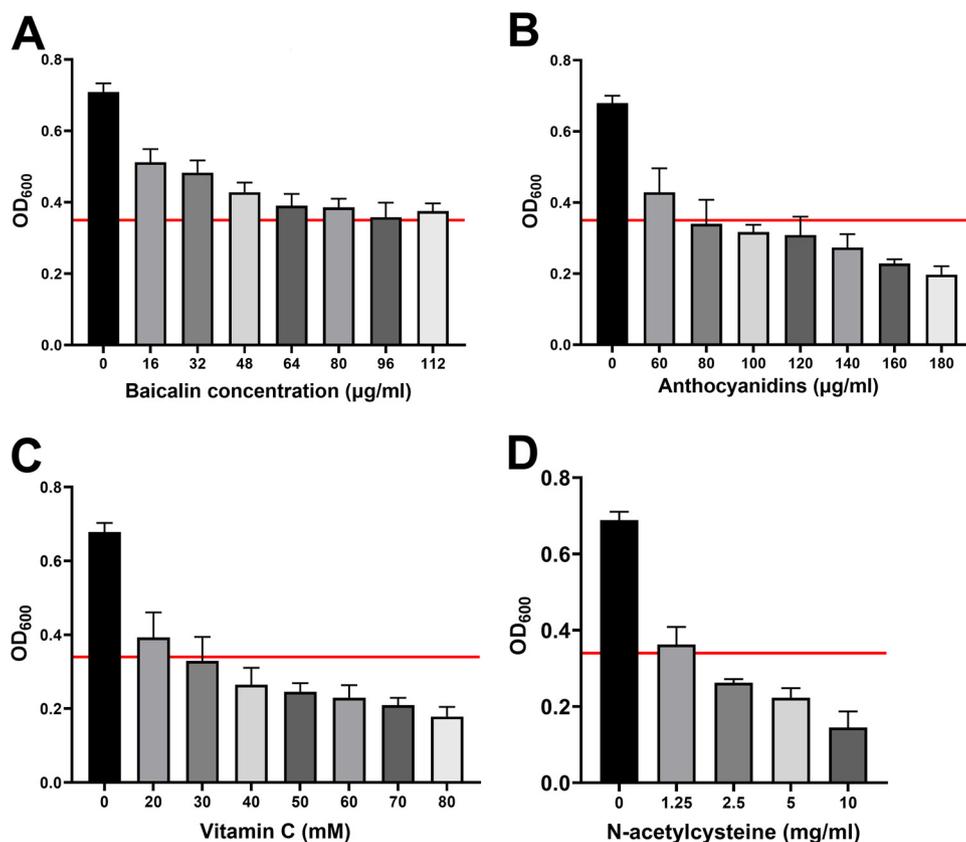
FIG 9 Effects of different antioxidants on biofilms of the wild-type strain. Biofilms grown for 3 days were treated with different concentrations of antioxidants for 24 h. The horizontal red line in each graph indicates a 50% reduction in the biomass of biofilms treated with antioxidants.

Δ*spoT* strain could not form a complete biofilm. This indicates that SpoT is involved in regulating the oxidative stress-induced formation of *H. pylori* biofilms.

NapA, which activates neutrophils, plays a major role in recruiting human neutrophils and monocytes to the infection site (49). Additionally, NapA stimulates the production of ROS in human neutrophils and monocytes (50). The sequence and structure of NapA are similar to those of Dps (DNA-binding protein from the starved cell) family proteins with iron-binding and DNA-protective activities (51). However, previous studies have demonstrated that the expression of NapA in *H. pylori* is not regulated by the iron content and that NapA is not involved in conferring metal resistance (52).

Proteins of the Dps family are expressed in most bacteria and accumulate under oxidative stress or nutrient starvation conditions. Some Dps family proteins protect the bacteria against oxidative stress (53).

The protective effect of NapA against oxidative stress was determined on the basis of upregulated NapA expression after the loss of the antioxidant enzyme AhpC (54). Upregulated NapA expression is the major pathway in *H. pylori* that compensates for the loss of major antioxidant stress factors (55). The survival rates of *H. pylori napA* mutants upon exposure to oxidative stress are lower than that of the WT strain, indicating that NapA protects *H. pylori* against oxidative stress damage (30). *H. pylori* NapA can bind DNA in the presence of iron ions. Therefore, the main role of NapA is to protect the DNA against iron-mediated oxidative stress damage (31). In this study, the Δ*napA* strain could hardly form a biofilm upon H_2O_2 stimulation but transformed into coccoid forms. Due to the lack of protection of the biofilm extracellular matrix, the genome of the Δ*napA* strain is more susceptible to H_2O_2 damage than the WT genome. In addition, there is evidence that the genomic DNA of the coccoid form of *H. pylori* is impaired by endogenous oxidative stress (56, 57).

A   (N-acetylcysteine)

5mg/ml   **10mg/ml**

B   (Vitamin C)

40mM   **80mM**
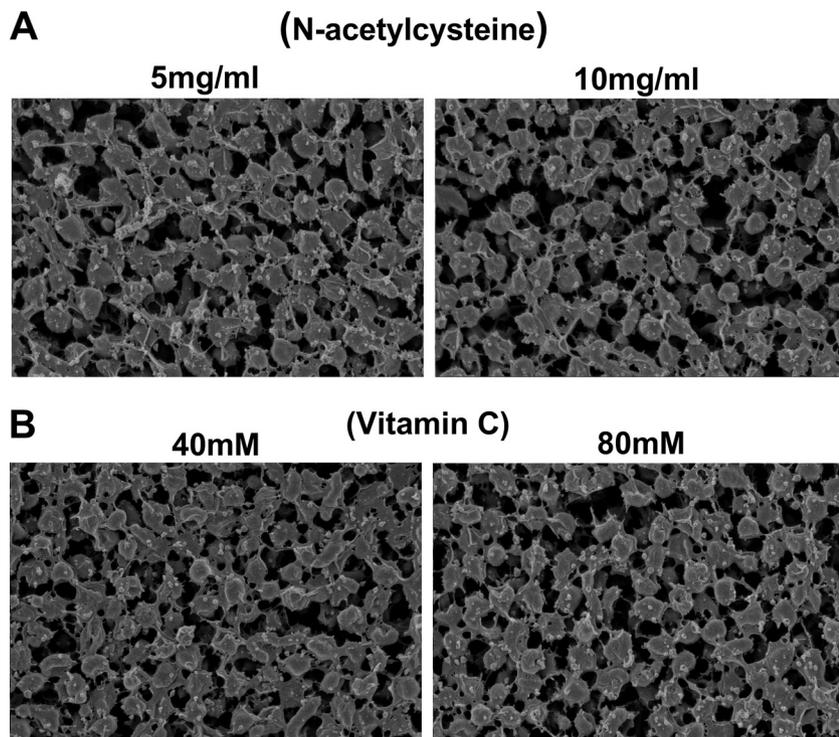
FIG 10 Scanning electron microscopy images of wild-type biofilms treated with different concentrations of *N*-acetylcysteine (A) or vitamin C (B) for 24 h.

Yang et al. have reported that NapA is involved in the formation of the extracellular matrix in *H. pylori* biofilms (58). The extracellular matrix of biofilms can prevent ROS diffusion (28). In this study, the biofilm formed by the Δ*napA* strain exhibited a thinner extracellular matrix and a higher number of cavities than those of the WT biofilm. Thus, ROS can penetrate the biofilm of the Δ*napA* strain.

An important mechanism by which (p)ppGpp induces global changes in transcription initiation involves the regulation of sigma factors. Under stringent environmental conditions, alternative sigma factors promote transcription, a process mediated by (p)ppGpp (42). In *H. pylori*, only two alternative σ factors (σ^{54} and σ^{28}) have been
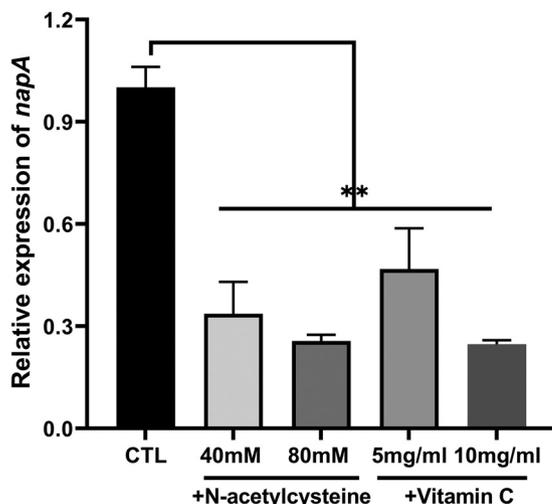
FIG 11 *napA* mRNA expression levels in the wild-type strain treated with different concentrations of vitamin C or *N*-acetylcysteine for 30 min. CTL, control.

reported (43). Previously, we had demonstrated that σ^{54} positively regulates NapA (59). Niehus et al. reported that the promoter sequence of σ^{54}-dependent genes is TTTGCTT (60). Analysis of the upstream sequence of the putative ATG start codon in the *napA* open reading frame did not reveal a similar conservative sequence. However, analysis of the upstream sequence of the putative ATG start codon in the σ^{28} open reading frame revealed a potential conserved sequence (TTTGCTT), which may be recognized by σ^{54} (see Fig. S3A in the supplemental material). This indicates that σ^{54} can upregulate σ^{28}. The expression levels of σ^{28} in the biofilm cells of the *H. pylori* WT and σ^{54} knockout strains were comparatively analyzed using qRT-PCR. σ^{28} expression was not upregulated in the σ^{54} knockout strain (Fig. S3B).

Josenhans et al. reported that the promoter sequence of genes regulated by σ^{28} is TAAAXXXXXXXXXXXXCCGAT (61). Analysis of the upstream sequence of the *napA* start codon revealed a similar conserved sequence (Fig. S4A). Therefore, σ^{28} may activate the transcription of *napA* by binding to its promoter. Comparative analysis of *napA* mRNA expression in the biofilm cells of the *H. pylori* WT and σ^{28} knockout strains revealed that *napA* expression was not upregulated in the σ^{28} knockout strain (Fig. S4B).

Further, σ^{54} expression levels in the biofilm cells of the WT, $\Delta spoT$, and $spoT^*$ strains were examined. The analysis revealed that SpoT can upregulate σ^{54} expression (Fig. S5).

Thus, SpoT could upregulate *napA* transcription by activating σ^{54}. Further, σ^{54} directly binds to the σ^{28} promoter to activate its transcription. σ^{28} subsequently promotes *napA* transcription by directly binding to the *napA* promoter and consequently facilitates the adaptation of *H. pylori* to the oxidative stress environment.

Previous studies have demonstrated that NAC can downregulate the production of the extracellular polysaccharide matrix and consequently inhibit the formation of biofilms in various bacteria (62). In this study, NAC inhibited the formation of *H. pylori* biofilms *in vitro* and exhibited antibiofilm activity. The administration of NAC before antibiotics can improve the clearance of drug-resistant *H. pylori* (11).

Various studies have demonstrated that Vc, a major dietary micronutrient, exerts growth-inhibitory effects against mycobacteria (63). Vc and NAC have been reported to synergistically potentiate the growth-inhibitory activity of antibiotics (64). Recent studies have reported that low concentrations of Vc exhibit antibiofilm activity in *Bacillus subtilis* by downregulating the synthesis of extracellular polymers (22). This may be attributed to the mucolytic activity of *N*-acetylcysteine or the structural homology between Vc and AI-2 (inhibition of AI-2-related quorum sensing) (5, 22). In this study, Vc and NAC exhibited similar anti-*H. pylori* biofilm activities. In addition to the reasons mentioned above, the downregulation of *napA* mRNA expression may be involved.

This study reported a novel mechanism of *H. pylori* biofilm formation under oxidative stress conditions. SpoT-regulated NapA promoted H_2O_2-induced biofilm formation in *H. pylori*.

MATERIALS AND METHODS

Bacterial strains, culture medium, and growth conditions. *H. pylori* strain 26695 was s kind gift from Zhang Jianzhong, Chinese Center for Disease Control and Prevention. The strain was resuscitated on Mueller-Hinton agar (Oxoid, England) containing 5% sterile sheep blood and was cultured in a microaerobic environment (5% O_2, 10% CO_2, and 85% N_2) at 37°C.

The liquid medium used to culture *H. pylori* was Brucella broth supplemented with 10% newborn calf serum. The bacteria were cultured at 37°C and 120 rpm in a shaker. The mutant strain and the complementation strain were cultured on agar plates containing 25 μg/ml kanamycin or 25 μg/ml chloramphenicol (both from Sigma-Aldrich, St. Louis, MO), respectively. These strains were stored in brain heart infusion medium (Oxoid, England) at −80°C with 20% (vol/vol) glycerol.

The clinical isolate H57 was isolated from a patient with a gastric ulcer at Qiannan People's Hospital in Guizhou Province. The patient's *H. pylori* infection was not alleviated even after three rounds of standard triple therapy. The patient signed an informed consent form before undergoing gastroscopy to isolate the bacteria. The study was approved by the Ethics Committee of the Shandong University School of Medicine (protocol number ECSBMSSDU2020-1-021).

The isolated *H. pylori* strains were identified on the basis of Gram staining and urease tests.

The TOP10 strain of *E. coli* (Tiangen, Beijing, China) was cultured in Luria-Bertani medium at 37°C.

Biofilm construction. Recent studies have demonstrated that low concentrations of oxidative stress-inducing agents can activate the bacterial stress response mechanism and stimulate the formation of

biofilms (33, 65). H_2O_2 was added (final concentration, $50\,\mu M$) to Brinell agar medium (at 50°C), which was then poured onto a petri plate. The bacteria were allowed to form a biofilm by the "colony biofilm" method (66).

A sterilized and dried nitrocellulose filter (NC) membrane ($1\,cm^2$) was placed on fresh Brinell solid medium. The log-phase culture of *H. pylori* was resuspended in Brinell liquid medium to adjust the initial optical density at 600 nm (OD_{600}) to 0.2. Next, $25\,\mu l$ of the bacterial suspension was inoculated onto the NC membrane and allowed to dry partially. The plates were incubated upside down in a three-gas constant-temperature incubator. The bacteria were cultured for 4 days at 37°C in a microaerobic environment (85% N_2, 10% CO_2, and 5% O_2).

Growth curve of the biofilm. The biofilm attached to the NC membrane was removed every 12 h and was washed repeatedly with sterile phosphate-buffered saline (PBS; pH 7) to obtain the planktonic bacteria attached to the surface of the biofilm. The cells in the biofilm were scraped and resuspended in 1 ml of liquid medium. The absorbance (expressed as the OD_{600}) of the suspension was measured. The experiment was repeated three times. The growth curve of the *H. pylori* biofilm was generated based on the absorbance values.

SEM. The samples were subjected to SEM by following the standard procedure. The biofilm was gently washed three times with autoclaved PBS to remove planktonic bacteria from the surface. Next, the bacterial cells were fixed in 2.5% glutaraldehyde for 2 h at 4°C, washed three times with coconut oleate buffer, and dehydrated in an ethanol series (25%, 50%, 75%, 95%, and 100%). The sample was freeze-dried, sputtered, gilded, and observed under a scanning electron microscope.

CLSM. The thickness of the biofilm was analyzed using CLSM. The mature biofilm was washed multiple times with PBS to remove the planktonic bacteria attached to the surface. The biofilm was incubated with a fluorescent dye (LIVE/DEAD BacLight bacterial viability kit; Invitrogen, USA) for 20 min in the dark. Next, the sample was washed with PBS and placed on a glass slide. The sample was then incubated with an appropriate amount of antiquench agent, sealed with gum, and observed under a confocal laser scanning microscope.

TLC. To determine the levels of (p)ppGpp in the planktonic and biofilm-forming bacteria, (p)ppGpp was labeled with ^{32}P. The planktonic and biofilm-forming cells were washed with PBS, and their OD_{600} values were adjusted to 0.2. The bacterial cells were centrifuged, and the supernatant was discarded. The cells were incubated with KH_2PO_4 and were labeled with $100\,\mu Ci/ml$ ^{32}P at 37°C and 120 rpm for 3 h. Next, the samples were centrifuged, rinsed, resuspended in $50\,\mu l$ of KH_2PO_4, incubated with an equal volume of 2 M formic acid, frozen at a low temperature, thawed at room temperature, and centrifuged at 13,000 rpm for 5 min after several freeze-thaw cycles. The supernatant ($2.5\,\mu l$) was spotted onto polyethyleneimine cellulose-coated plates. The sample was dried and subjected to chromatography with 1.5 M KH_2PO_4 for 1 to 2 h. The chromatographic plate was dried in a fume hood. The phosphor screen was developed overnight and scanned.

Evaluation of antibiotic sensitivity. The sensitivities of *H. pylori* to various antibiotics were evaluated using the agar dilution method reported by Osato et al. (67). The following six antibiotics were used to evaluate the antibiotic sensitivities of different strains: penicillin G, amoxicillin, clarithromycin, tetracycline hydrochloride, ciprofloxacin, and metronidazole.

The planktonic bacterial culture (OD_{600}, 0.8) was plated onto agar plates containing 2-fold serial dilutions of antibiotics. All plates were incubated at 37°C for 48 h under microaerobic conditions. The MIC and minimal bactericidal concentration (MBC) values were determined.

To evaluate the antibiotic sensitivities of biofilm-forming bacteria, the mature biofilms attached to the NC membranes were incubated for 12 h in liquid media containing different concentrations of antibiotics. The bacterial cells were washed three times with PBS and were resuspended in the liquid medium. The bacterial suspension (OD_{600}, 0.8) was inoculated onto agar plates without antibiotics and was incubated at 37°C for 48 h to determine the MIC and MBC values.

To determine the sensitivities of bacteria to different antibiotics, a colony-forming assay was performed. Bacteria were cultured in liquid culture medium (approximately 10^8 CFU/ml). The bacterial suspension serially diluted in PBS ($5\,\mu l$) was plated onto Mueller-Hinton agar medium containing 5% sterile sheep blood and inhibitory concentrations of the antibiotics to allow the formation of a lawn. The bacteria were cultured in a microaerobic environment (5% O_2, 10% CO_2, and 85% N_2) at 37°C for 3 days. The CFU of different strains were recorded. All experiments were performed at least three times.

Evaluation of the effects of antioxidants on *H. pylori* biofilms. The effects of antioxidants (baicalin, Vc, anthocyanin, and NAC) on *H. pylori* biofilms were examined. Biofilms grown for 3 days were treated with different concentrations of antioxidants for 24 h. The biofilm without antioxidant treatment was used as a control. Next, the biofilms were washed three times with sterile water to remove loosely attached bacteria and were dried at room temperature for 30 min.

Samples for SEM analysis were prepared by a standard procedure. The biofilm was stained with 1% crystal violet for 5 min, washed five times with sterile water to remove excess dye, and dried at 25°C for 1 h. Next, the stain was solubilized using absolute ethanol (1 ml) for 15 min. The absorbance of the solution ($200\,\mu l$) at 600 nm was measured.

mRNA sequencing. mRNA high-throughput sequencing service was provided by CloudSeq Biotech (Shanghai, China). The *H. pylori* WT and $\Delta spoT$ strains cultured to the logarithmic phase or those that had formed biofilms were collected and divided into the following four groups according to the physiological state of the bacteria: WtP, WtB, $\Delta spoT$P, and $\Delta spoT$B cells. The bacterial cells were collected three times independently in each group.

The rRNAs in total RNA ($1\,\mu g$) were removed by using Ribo-Zero rRNA removal kits (Illumina, San Diego, CA, USA) according to the manufacturer's instructions. RNA libraries were constructed with

rRNA-free RNA by using the TruSeq Stranded Total RNA library prep kit (Illumina, San Diego, CA, USA) according to the manufacturer's instructions. The quality and quantity of the libraries were determined using the Bioanalyzer 2100 system (Agilent Technologies, Inc., USA). The libraries (10 pM) were denatured, captured on Illumina flow cells, amplified *in situ* as clusters, and subjected to 150-cycle sequencing on an Illumina HiSeq sequencer according to the manufacturer's instructions. The quality of paired-end reads was determined using Q30. The 3′-end adaptor was trimmed, and low-quality reads were removed using Cutadapt software (v1.9.1). Next, the high-quality trimmed reads (clean reads) were aligned with the *H. pylori* 26695 reference genome (ASM852v1) using HISAT2 software (v2.0.4). Based on the Ensembl gene annotation file, the gene expression level (expressed as fragments per kilobase per million mapped reads [FPKM]) was analyzed using Cuffdiff software (part of Cufflinks). The fold change in expression level and the *P* value were calculated based on FPKM to identify the differentially expressed mRNAs.

RNA extraction and qRT-PCR. Total bacterial RNA was extracted using the TRIzol reagent (Invitrogen, Carlsbad, CA, USA) and was reverse transcribed into cDNA using the PrimeScript RT kit (TaKaRa, Otsu, Shiga, Japan). The reaction mixture comprised 2.5 μl diluted cDNA, 0.4 μl primer mixture, 5 μl TB green *Premix Ex Taq* (TaKaRa), and 2.1 μl double-distilled water. qRT-PCR analysis was performed using an ABI Prism 7500 sequence detection system (Applied Biosystems, Carlsbad, CA). The dissociation curve was analyzed to verify the homogeneity of the product. The analysis was repeated three times. The internal reference gene for qRT-PCR analysis was 16S rRNA. The expression levels of the target genes were analyzed using the $\Delta\Delta C_T$ method.

Construction of *napA* and *spoT* knockout and complementation strains. Previously, we had successfully constructed the Δ*spoT* and *spoT** strains (29). The plasmids (pILL570 and pUC18K2) used to construct mutants were provided by Agnès Labigne (Pasteur Institute).

The method of construction of the Δ*napA* strain was identical to that of the Δ*spoT* strain. Briefly, *napA* in the *H. pylori* 26695 genome was inactivated by the insertion of *aphA-3* (encoding kanamycin).

The *napA* complementation (*napA**) strain was constructed by inserting WT *napA* between *hp0203* and *hp0204*, which contain the untranslated regions of the *H. pylori* chromosome. Briefly, *napA* along with the promoter region was PCR amplified and cloned into the PstI and XhoI sites of pBHKP252 (provided by Bi Hongkai of Nanjing Medical University). The recombinant plasmid was introduced into the Δ*napA* strain through natural transformation, and the recombinant colonies were isolated on Columbia blood agar plates containing chloramphenicol (10 μg/ml). Finally, the successful construction of the *napA** strain was verified using PCR and sequencing. The primers used in this experiment are shown in Table S2.

WGCNA. A WGCNA network (68) was generated using the following four sets of transcriptome data: WtP ($n = 3$), WtB ($n = 3$), Δ*spoT*P ($n = 3$), and Δ*spoT*B strain ($n = 3$). A consensus network along with module statistics was generated by following the method of Langfelder et al. (69). The similarity matrix was calculated from the *H. pylori* transcriptome data based on the Pearson correlation coefficient. The exponential function was used as the adjacency function to determine the optimal parameters of the adjacency function according to the size of the transformed adjacency matrix R^2, which results in strong biological significance. The topological overlap metric (TOM) (70) is derived from the adjacency matrix. Cluster analysis was performed on the results of gene clustering. The height of the hierarchical cluster tree was adjusted so that the smallest module contained at least 20 genes. The correlation between the gene module and the sample clinical indication matrix was analyzed. The correlation between each clinical indication and each module was calculated. The module with the strongest correlation with the target clinical indication was selected. Furthermore, the module was considered significant when the *P* value was <0.05. The most significant module (color coded red in Fig. 4B) of 24 genes with WGCNA edge weights of >0.10 was represented using Cytoscape, v3.1 (71).

Statistical analysis. Data are presented as means ± standard errors of the means. Statistical significance was determined using the unpaired Student *t* test, and the *P* values were corrected by the Sidak-Bonferroni method for multiple comparisons. *P* values of <0.05 were considered statistically significant. The results were analyzed using GraphPad Prism software (GraphPad Software Inc., La Jolla, CA, USA).

Data availability. The data supporting the findings are presented in the article and have been deposited in the NCBI database (BioProject accession no. PRJNA648673 and BioSample accession no. SAMN15644285 to SAMN15644288). The other relevant files can be acquired from the authors upon request.

SUPPLEMENTAL MATERIAL

Supplemental material is available online only.
SUPPLEMENTAL FILE 1, PDF file, 0.5 MB.

Y.S., W.L., and J.J. designed the study. Y.Z., Y.C., and H.L. performed the experimental work. Z.C., Y.S., and Z.X. analyzed the data. All authors contributed to the data interpretation and the writing of the paper.

We declare no competing interests.

REFERENCES

1. Mentis A, Lehours P, Mégraud F. 2015. Epidemiology and diagnosis of Helicobacter pylori infection. Helicobacter 20(Suppl 1):1–7. https://doi.org/10.1111/hel.12250.
2. Sipponen P, Hyvärinen H. 1993. Role of Helicobacter pylori in the pathogenesis of gastritis, peptic ulcer and gastric cancer. Scand J Gastroenterol 28:3–6. https://doi.org/10.3109/00365529309098333.
3. Doorakkers E, Lagergren J, Engstrand L, Brusselaers N. 2016. Eradication of Helicobacter pylori and gastric cancer: a systematic review and meta-analysis of cohort studies. J Natl Cancer Inst 108:djw132. https://doi.org/10.1093/jnci/djw132.
4. Savoldi A, Carrara E, Graham DY, Conti M, Tacconelli E. 2018. Prevalence of antibiotic resistance in Helicobacter pylori: a systematic review and meta-analysis in World Health Organization regions. Gastroenterology 155:1372–1382. https://doi.org/10.1053/j.gastro.2018.07.007.
5. Hathroubi S, Servetas SL, Windham I, Merrell DS, Ottemann KM. 2018. Helicobacter pylori biofilm formation and its potential role in pathogenesis. Microbiol Mol Biol Rev 82:e00001-18. https://doi.org/10.1128/MMBR.00001-18.
6. Krzyżek P, Grande R, Migdał P, Paluch E, Gościniak G. 2020. Biofilm formation as a complex result of virulence and adaptive responses of Helicobacter pylori. Pathogens 9:1062. https://doi.org/10.3390/pathogens9121062.
7. Yonezawa H, Osaki T, Kamiya S. 2015. Biofilm formation by Helicobacter pylori and its involvement for antibiotic resistance. Biomed Res Int 2015:914791. https://doi.org/10.1155/2015/914791.
8. Ge X, Cai Y, Chen Z, Gao S, Geng X, Li Y, Li Y, Jia J, Sun Y. 2018. Bifunctional enzyme SpoT is involved in biofilm formation of Helicobacter pylori with multidrug resistance by upregulating efflux pump Hp1174 (gluP). Antimicrob Agents Chemother 62:e00957-18. https://doi.org/10.1128/AAC.00957-18.
9. Carron MA, Tran VR, Sugawa C, Coticchia JM. 2006. Identification of Helicobacter pylori biofilms in human gastric mucosa. J Gastrointest Surg 10:712–717. https://doi.org/10.1016/j.gassur.2005.10.019.
10. Coticchia J, Sugawa C, Tran V, Gurrola J, Kowalski E, Carron M. 2006. Presence and density of Helicobacter pylori biofilms in human gastric mucosa in patients with peptic ulcer disease. J Gastrointest Surg 10:883–889. https://doi.org/10.1016/j.gassur.2005.12.009.
11. Cammarota G, Branca G, Ardito F, Sanguinetti M, Ianiro G, Cianci R, Torelli R, Masala G, Gasbarrini A, Fadda G, Landolfi R, Gasbarrini G. 2010. Biofilm demolition and antibiotic treatment to eradicate resistant Helicobacter pylori: a clinical trial. Clin Gastroenterol Hepatol 8:817–820.e3. https://doi.org/10.1016/j.cgh.2010.05.006.
12. Sigal M, Rothenberg ME, Logan CY, Lee JY, Honaker RW, Cooper RL, Passarelli B, Camorlinga M, Bouley DM, Alvarez G, Nusse R, Torres J, Amieva MR. 2015. Helicobacter pylori activates and expands Lgr5$^+$ stem cells through direct colonization of the gastric glands. Gastroenterology 148:1392–1404.e21. https://doi.org/10.1053/j.gastro.2015.02.049.
13. Carrillo JLM, García FPC, Coronado OG, García MAM, Cordero JFC. 2017. Physiology and pathology of innate immune response against pathogens. *In* Rezaei N (ed), Physiology and pathology of immunology. IntechOpen Limited, London, United Kingdom. https://doi.org/10.5772/intechopen.70556.
14. Davies GR, Simmonds NJ, Stevens TRJ, Sheaff MT, Banatvala N, Laurenson IF, Blake DR, Rampton DS. 1994. Helicobacter pylori stimulates antral mucosal reactive oxygen metabolite production in vivo. Gut 35:179–185. https://doi.org/10.1136/gut.35.2.179.
15. Bagchi D, Bhattacharya G, Stohs SJ. 1996. Production of reactive oxygen species by gastric cells in association with Helicobacter pylori. Free Radic Res 24:439–450. https://doi.org/10.3109/10715769609088043.
16. Ramarao N, Gray-Owen SD, Meyer TF. 2000. Helicobacter pylori induces but survives the extracellular release of oxygen radicals from professional phagocytes using its catalase activity. Mol Microbiol 38:103–113. https://doi.org/10.1046/j.1365-2958.2000.02114.x.
17. Handa O, Naito Y, Yoshikawa T. 2011. Redox biology and gastric carcinogenesis: the role of Helicobacter pylori. Redox Rep 16:1–7. https://doi.org/10.1179/174329211X12968219310756.
18. Wang G, Alamuri P, Maier RJ. 2006. The diverse antioxidant systems of Helicobacter pylori. Mol Microbiol 61:847–860. https://doi.org/10.1111/j.1365-2958.2006.05302.x.
19. Gambino M, Cappitelli F. 2016. Biofilm responses to oxidative stress. Biofouling 32:167–178. https://doi.org/10.1080/08927014.2015.1134515.
20. Kadkhodaei S, Siavoshi F, Noghabi KA. 2020. Mucoid and coccoid Helicobacter pylori with fast growth and antibiotic resistance. Helicobacter 25:e12678. https://doi.org/10.1111/hel.12678.
21. Yang-Ou YB, Hu Y, Zhu Y, Lu NH. 2018. The effect of antioxidants on Helicobacter pylori eradication: a systematic review with meta-analysis. Helicobacter 23:e12535. https://doi.org/10.1111/hel.12535.
22. Pandit S, Ravikumar V, Abdel-Haleem AM, Derouiche A, Mokkapati VRSS, Sihlbom C, Mineta K, Gojobori T, Gao X, Westerlund F, Mijakovic I. 2017. Low concentrations of vitamin C reduce the synthesis of extracellular polymers and destabilize bacterial biofilms. Front Microbiol 8:2599. https://doi.org/10.3389/fmicb.2017.02599.
23. Chen L, Keramati L, Helmann JD. 1995. Coordinate regulation of Bacillus subtilis peroxide stress genes by hydrogen peroxide and metal ions. Proc Natl Acad Sci U S A 92:8190–8194. https://doi.org/10.1073/pnas.92.18.8190.
24. Scherr TD, Roux CM, Hanke ML, Angle A, Dunman PM, Kielian T. 2013. Global transcriptome analysis of Staphylococcus aureus biofilms in response to innate immune cells. Infect Immun 81:4363–4376. https://doi.org/10.1128/IAI.00819-13.
25. Kulkarni R, Antala S, Wang A, Amaral FE, Rampersaud R, LaRussa SJ, Planet PJ, Ratner AJ. 2012. Cigarette smoke increases Staphylococcus aureus biofilm formation via oxidative stress. Infect Immun 80:3804–3811. https://doi.org/10.1128/IAI.00689-12.
26. Hauryliuk V, Atkinson GC, Murakami KS, Tenson T, Gerdes K. 2015. Recent functional insights into the role of (p)ppGpp in bacterial physiology. Nat Rev Microbiol 13:298–309. https://doi.org/10.1038/nrmicro3448.
27. Gentry DR, Cashel M. 1996. Mutational analysis of the Escherichia coli spoT gene identifies distinct but overlapping regions involved in ppGpp synthesis and degradation. Mol Microbiol 19:1373–1384. https://doi.org/10.1111/j.1365-2958.1996.tb02480.x.
28. Flemming H-C, Wingender J, Szewzyk U, Steinberg P, Rice SA, Kjelleberg S. 2016. Biofilms: an emergent form of bacterial life. Nat Rev Microbiol 14:563–575. https://doi.org/10.1038/nrmicro.2016.94.
29. Geng X, Li W, Chen Z, Gao S, Hong W, Ge X, Hou G, Hu Z, Zhou Y, Zeng B, Li W, Jia J, Sun Y. 2017. The bifunctional enzyme SpoT is involved in the clarithromycin tolerance of Helicobacter pylori by upregulating the transporters HP0939, HP1017, HP0497, and HP0471. Antimicrob Agents Chemother 61:e02011-16. https://doi.org/10.1128/AAC.02011-16.
30. Cooksley C, Jenks PJ, Green A, Cockayne A, Logan RPH, Hardie KR. 2003. NapA protects Helicobacter pylori from oxidative stress damage, and its production is influenced by the ferric uptake regulator. J Med Microbiol 52:461–469. https://doi.org/10.1099/jmm.0.05070-0.
31. Wang G, Hong Y, Olczak A, Maier SE, Maier RJ. 2006. Dual roles of Helicobacter pylori NapA in inducing and combating oxidative stress. Infect Immun 74:6839–6846. https://doi.org/10.1128/IAI.00991-06.
32. Dey A, Lakshmanan J. 2013. The role of antioxidants and other agents in alleviating hyperglycemia mediated oxidative stress and injury in liver. Food Funct 4:1148–1184. https://doi.org/10.1039/c3fo30317a.
33. Jang IA, Kim J, Park W. 2016. Endogenous hydrogen peroxide increases biofilm formation by inducing exopolysaccharide production in Acinetobacter oleivorans DR1. Sci Rep 6:21121. https://doi.org/10.1038/srep21121.
34. Ranieri MR, Whitchurch CB, Burrows LL. 2018. Mechanisms of biofilm stimulation by subinhibitory concentrations of antimicrobials. Curr Opin Microbiol 45:164–169. https://doi.org/10.1016/j.mib.2018.07.006.
35. Jolivet-Gougeon A, Bonnaure-Mallet M. 2014. Biofilms as a mechanism of bacterial resistance. Drug Discov Today Technol 11:49–56. https://doi.org/10.1016/j.ddtec.2014.02.003.
36. Hassett DJ, Ma JF, Elkins JG, McDermott TR, Ochsner UA, West SE, Huang CT, Fredericks J, Burnett S, Stewart PS, McFeters G, Passador L, Iglewski BH. 1999. Quorum sensing in Pseudomonas aeruginosa controls expression of catalase and superoxide dismutase genes and mediates biofilm

susceptibility to hydrogen peroxide. Mol Microbiol 34:1082–1093. https://doi.org/10.1046/j.1365-2958.1999.01672.x.

37. Halliwell B, Clement MV, Long LH. 2000. Hydrogen peroxide in the human body. FEBS Lett 486:10–13. https://doi.org/10.1016/s0014-5793(00)02197-9.

38. Collins KD, Andermann TM, Draper J, Sanders L, Williams SM, Araghi C, Ottemann KM. 2016. The Helicobacter pylori CZB cytoplasmic chemo-receptor TlpD forms an autonomous polar chemotaxis signaling complex that mediates a tactic response to oxidative stress. J Bacteriol 198:1563–1575. https://doi.org/10.1128/JB.00071-16.

39. Perkins A, Tudorica DA, Amieva MR, Remington SJ, Guillemin K. 2019. Helicobacter pylori senses bleach as a chemoattractant using a cytosolic chemoreceptor. bioRxiv https://doi.org/10.1101/544239.

40. Barnard FM, Loughlin MF, Fainberg HP, Messenger MP, Ussery DW, Williams P, Jenks PJ. 2004. Global regulation of virulence and the stress response by CsrA in the highly adapted human gastric pathogen Helicobacter pylori. Mol Microbiol 51:15–32. https://doi.org/10.1046/j.1365-2958.2003.03788.x.

41. Mouery K, Rader BA, Gaynor EC, Guillemin K. 2006. The stringent response is required for Helicobacter pylori survival of stationary phase, exposure to acid, and aerobic shock. J Bacteriol 188:5494–5500. https://doi.org/10.1128/JB.00366-06.

42. Potrykus K, Cashel M. 2008. (p)ppGpp: still magical? Annu Rev Microbiol 62:35–51. https://doi.org/10.1146/annurev.micro.62.081307.162903.

43. Tomb JF, White O, Kerlavage AR, Clayton RA, Sutton GG, Fleischmann RD, Ketchum KA, Klenk HP, Gill S, Dougherty BA, Nelson K, Quackenbush J, Zhou L, Kirkness EF, Peterson S, Loftus B, Richardson D, Dodson R, Khalak HG, Glodek A, McKenney K, Fitzegerald LM, Lee N, Adams MD, Hickey EK, Berg DE, Gocayne JD, Utterback TR, Peterson JD, Kelley JM, Cotton MD, Weidman JM, Fujii C, Bowman C, Watthey L, Wallin E, Hayes WS, Borodovsky M, Karp PD, Smith HO, Fraser CM, Venter JC. 1997. The complete genome sequence of the gastric pathogen Helicobacter pylori. Nature 388:539–547. https://doi.org/10.1038/41483.

44. Wells DH, Gaynor EC. 2006. Helicobacter pylori initiates the stringent response upon nutrient and pH downshift. J Bacteriol 188:3726–3729. https://doi.org/10.1128/JB.188.10.3726-3729.2006.

45. Chávez de Paz LE, Lemos JA, Wickström D, Sedgley CM. 2012. Role of (p)ppGpp in biofilm formation by Enterococcus faecalis. Appl Environ Microbiol 78:1627–1630. https://doi.org/10.1128/AEM.07036-11.

46. Sugisaki K, Hanawa T, Yonezawa H, Osaki T, Fukutomi T, Kawakami H, Yamamoto T, Kamiya S. 2013. Role of (p)ppGpp in biofilm formation and expression of filamentous structures in Bordetella pertussis. Microbiology (Reading) 159:1379–1389. https://doi.org/10.1099/mic.0.066597-0.

47. He H, Cooper JN, Mishra A, Raskin DM. 2012. Stringent response regulation of biofilm formation in Vibrio cholerae. J Bacteriol 194:2962–2972. https://doi.org/10.1128/JB.00014-12.

48. Nunes-Alves C. 2014. Targeting (p)ppGpp disrupts biofilms. Nat Rev Microbiol 12:461. https://doi.org/10.1038/nrmicro3302.

49. Brisslert M, Enarsson K, Lundin S, Karlsson A, Kusters JG, Svennerholm AM, Backert S, Quiding-Järbrink M. 2005. Helicobacter pylori induce neutrophil transendothelial migration: role of the bacterial HP-NAP. FEMS Microbiol Lett 249:95–103. https://doi.org/10.1016/j.femsle.2005.06.008.

50. Satin B, Del Giudice G, Della Bianca V, Dusi S, Laudanna C, Tonello F, Kelleher D, Rappuoli R, Montecucco C, Rossi F. 2000. The neutrophil-activating protein (HP-NAP) of Helicobacter pylori is a protective antigen and a major virulence factor. J Exp Med 191:1467–1476. https://doi.org/10.1084/jem.191.9.1467.

51. Larsson NG, Wang J, Wilhelmsson H, Oldfors A, Rustin P, Lewandoski M, Barsh GS, Clayton DA. 1998. Mitochondrial transcription factor A is necessary for mtDNA maintenance and embryogenesis in mice. Nat Genet 18:231–236. https://doi.org/10.1038/ng0398-231.

52. Dundon WG, Nishioka H, Polenghi A, Papinutto E, Zanotti G, Montemurro P, Del Giudice G, Rappuoli R, Montecucco C. 2002. The neutrophil-activating protein of Helicobacter pylori. Int J Med Microbiol 291:545–550. https://doi.org/10.1078/1438-4221-00165.

53. Nair S, Finkel SE. 2004. Dps protects cells against multiple stresses during stationary phase. J Bacteriol 186:4192–4198. https://doi.org/10.1128/JB.186.13.4192-4198.2004.

54. Olczak AA, Olson JW, Maier RJ. 2002. Oxidative-stress resistance mutants of Helicobacter pylori. J Bacteriol 184:3186–3193. https://doi.org/10.1128/jb.184.12.3186-3193.2002.

55. Olczak AA, Wang G, Maier RJ. 2005. Up-expression of NapA and other oxidative stress proteins is a compensatory response to loss of major Helicobacter pylori stress resistance factors. Free Radic Res 39:1173–1182. https://doi.org/10.1080/10715760500306729.

56. Andersen LP, Rasmussen L. 2009. Helicobacter pylori—coccoid forms and biofilm formation. FEMS Immunol Med Microbiol 56:112–115. https://doi.org/10.1111/j.1574-695X.2009.00556.x.

57. Narikawa S, Kawai S, Aoshima H, Kawamata O, Kawaguchi R, Hikiji K, Kato M, Iino S, Mizushima Y. 1997. Comparison of the nucleic acids of helical and coccoid forms of Helicobacter pylori. Clin Diagn Lab Immunol 4:285–290. https://doi.org/10.1128/CDLI.4.3.285-290.1997.

58. Yang FL, Hassanbhai AM, Chen HY, Huang ZY, Lin TL, Wu SH, Ho B. 2011. Proteomannans in biofilm of Helicobacter pylori ATCC 43504. Helicobacter 16:89–98. https://doi.org/10.1111/j.1523-5378.2010.00815.x.

59. Sun Y, Liu S, Li W, Shan Y, Li X, Lu X, Li Y, Guo Q, Zhou Y, Jia J. 2013. Proteomic analysis of the function of sigma factor σ^{54} in Helicobacter pylori survival with nutrition deficiency stress in vitro. PLoS One 8:e72920. https://doi.org/10.1371/journal.pone.0072920.

60. Niehus E, Gressmann H, Ye F, Schlapbach R, Dehio M, Dehio C, Stack A, Meyer TF, Suerbaum S, Josenhans C. 2004. Genome-wide analysis of transcriptional hierarchy and feedback regulation in the flagellar system of Helicobacter pylori. Mol Microbiol 52:947–961. https://doi.org/10.1111/j.1365-2958.2004.04006.x.

61. Josenhans C, Niehus E, Amersbach S, Hörster A, Betz C, Drescher B, Hughes KT, Suerbaum S. 2002. Functional characterization of the antagonistic flagellar late regulators FliA and FlgM of Helicobacter pylori and their effects on the H. pylori transcriptome. Mol Microbiol 43:307–322. https://doi.org/10.1046/j.1365-2958.2002.02765.x.

62. Dinicola S, De Grazia S, Carlomagno G, Pintucci JP. 2014. N-acetylcysteine as powerful molecule to destroy bacterial biofilms. A systematic review. Eur Rev Med Pharmacol Sci 18:2942–2948.

63. Vilchèze C, Hartman T, Weinrick B, Jacobs WR. 2013. Mycobacterium tuberculosis is extraordinarily sensitive to killing by a vitamin C-induced Fenton reaction. Nat Commun 4:1181. https://doi.org/10.1038/ncomms2898.

64. Khameneh B, Fazly Bazzaz BS, Amani A, Rostami J, Vahdati-Mashhadian N. 2016. Combination of anti-tuberculosis drugs with vitamin C or NAC against different Staphylococcus aureus and Mycobacterium tuberculosis strains. Microb Pathog 93:83–87. https://doi.org/10.1016/j.micpath.2015.11.006.

65. Yin S, Jiang B, Huang G, Gong Y, You B, Yang Z, Chen Y, Chen J, Yuan Z, Li M, Hu F, Zhao Y, Peng Y. 2017. Burn serum increases Staphylococcus aureus biofilm formation via oxidative stress. Front Microbiol 8:1191. https://doi.org/10.3389/fmicb.2017.01191.

66. Franklin MJ, Bothner B, Akiyama T, Chang C. 2015. New technologies for studying biofilms. Microbiol Spectr 3(4):MB-0016-2014. https://doi.org/10.1128/microbiolspec.MB-0016-2014.

67. Osato MS, Reddy R, Reddy SG, Penland RL, Graham DY. 2001. Comparison of the Etest and the NCCLS-approved agar dilution method to detect metronidazole and clarithromycin resistant Helicobacter pylori. Int J Antimicrob Agents 17:39–44. https://doi.org/10.1016/S0924-8579(00)00320-4.

68. Langfelder P, Horvath S. 2008. WGCNA: an R package for weighted correlation network analysis. BMC Bioinformatics 9:559. https://doi.org/10.1186/1471-2105-9-559.

69. Langfelder P, Zhang B, Horvath S. 2008. Defining clusters from a hierarchical cluster tree: the Dynamic Tree Cut package for R. Bioinformatics 24:719–720. https://doi.org/10.1093/bioinformatics/btm563.

70. Yip AM, Horvath S. 2007. Gene network interconnectedness and the generalized topological overlap measure. BMC Bioinformatics 8:22. https://doi.org/10.1186/1471-2105-8-22.

71. Saito R, Smoot ME, Ono K, Ruscheinski J, Wang PL, Lotia S, Pico AR, Bader GD, Ideker T. 2012. A travel guide to Cytoscape plugins. Nat Methods 9:1069–1076. https://doi.org/10.1038/nmeth.2212.